RSC Advances

PAPER

View Article Online
View Journal | View Issue

Cite this: *RSC Adv.*, 2020, **10**, 15383

Received 5th March 2020
Accepted 26th March 2020

DOI: 10.1039/d0ra02647f

rsc.li/rsc-advances

Room-temperature preparation of a chiral covalent organic framework for the selective adsorption of amino acid enantiomers†

Fang Liu,[bc] Hai-Long Qian,*[bc] Cheng Yang[bc] and Xiu-Ping Yan*[abcd]

Herein, we have reported the facile room-temperature synthesis of a chiral covalent organic framework (CCOF) for the enantioselective adsorption of amino acids. The prepared CCOF provides various stereoscopic interactions with amino acids for highly selective adsorption of their enantiomers.

Chirality is one of the most common properties of natural compounds including proteins, polysaccharides, nucleic acids and enzymes, and it plays an extremely important role in life activities.[1,2] However, the selective recognition and interaction of their enantiomers with organisms make a huge difference in activity, toxicity, adsorption, transfer, metabolism and elimination. Therefore, the exploration of efficient ways to obtain pure enantiomers becomes more and more urgent; however, this is highly challenging owing to the dramatic similarity of the physicochemical properties of two enantiomers.[3,4] To date, various chiral separation techniques have been proposed such as chromatography,[5,6] crystallization[7,8] and extraction.[9,10] Adsorption separation based on porous materials has shown advantages due to their strong chiral recognition ability, long-term stability, and less complexity.[11]

The exploration of chiral-functionalized porous materials as adsorbents for the highly efficient resolution of enantiomers has received extensive attention; these materials include metal–organic frameworks,[12,13] porous organic cages,[14,15] metal–organic cages[16,17] and composite porous materials.[18] However, the type of adsorbents for enantioselective adsorption was far more enough due to its challengeable preparation. As a consequence, it is necessary to design and prepare more new adsorbents with excellent stability and rapid kinetics for the selective adsorption of enantiomers.

Covalent organic frameworks (COFs)[19,20] are crystalline organic porous materials with broad applications in diverse fields including chromatography separation,[21,22] heterogeneous catalysis,[23,24] fluorescence sensing[25,26] and optoelectronic materials.[27,28] The large surface area, excellent stability and the number of duplicate ordered units of COFs allow numerous interactions between the host and guests, such as hydrogen bonding, π–π interactions, hydrophobic interactions and molecular sieving, indicating COFs as a convenient platform for enantioselective adsorption. Chiral covalent organic frameworks (CCOFs) have been explored as the stationary phase in chiral chromatography and as catalysts in asymmetric catalysis.[29–31] However, the application of CCOFs as adsorbents for selective adsorption has been rarely reported.

Here, we have reported the design and room-temperature (RT) synthesis of a CCOF, CTzDa, *via* the post-modification of the COF TzDa for the selective adsorption of the enantiomers of amino acids (AAs). TzDa consisting of 4,4′,4'-(1,3,5-triazine-2,4,6-triyl)trianiline (Tz) and 1,4-dihydroxyterephthalaldehyde (Da) was chosen as the platform for the preparation of chiral COF due to its high stability, easy synthesis and abundant active groups (–OH).[32] D-Camphoric acid was converted to its acid chloride to react with the hydroxyl group of TzDa for obtaining CTzDa. The application of CTzDa as the adsorbent for the chiral separation of AAs was further investigated *via* detailed experimental characterizations and computational modeling. This work shows high potential of chiral COFs as adsorbents in enantioselective adsorption.

The COFs used as adsorbents should possess great stability, high crystallinity and large surface areas. Moreover, the introduction of a chiral environment into the COF structure *via* a post-modification strategy is a widely accessible way to prepare CCOFs. In this work, TzDa, which possessed a highly ordered and stable structure with abundant active groups (–OH) for further modification, was chosen as the COF platform for preparing CCOF. As shown in Fig. 1, we synthesized TzDa by condensing Tz and Da at RT instead of high temperature and pressure (Fig. S1, ESI†).

[a]*State Key Laboratory of Food Science and Technology, Jiangnan University, Wuxi 214122, China. E-mail: xpyan@jiangnan.edu.cn*

[b]*International Joint Laboratory on Food Safety, Jiangnan University, Wuxi 214122, China. E-mail: hlqian@jiangnan.edu.cn*

[c]*Institute of Analytical Food Safety, School of Food Science and Technology, Jiangnan University, Wuxi 214122, China*

[d]*Key Laboratory of Synthetic and Biological Colloids, Ministry of Education, Jiangnan University, Wuxi 214122, China*

† Electronic supplementary information (ESI) available. See DOI: 10.1039/d0ra02647f

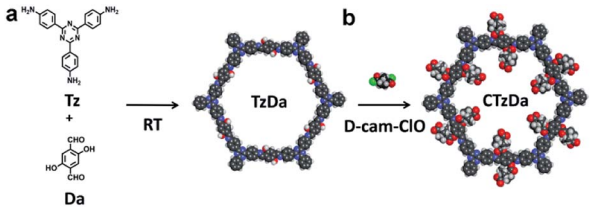

Fig. 1 Room-temperature synthesis: (a) TzDa; (b) CTzDa.

D-Camphor acid chloride (D-cam-ClO) (Fig. S2 and S3, ESI†) prepared from D-camphor acid was then applied to react with hydroxyl groups to introduce the chiral moiety into the channel of TzDa for preparing CTzDa.

The Fourier transform infrared (FTIR) spectra of TzDa show the C=N peak at 1665 cm^{-1} along with the disappearance of the peaks for the C=O and NH_2 bonds for the starting materials, indicating the successful condensation of Tz and Da (Fig. S4, ESI†). Compared with TzDa, CTzDa exhibited additional peaks at 1805 cm^{-1}, 1741 cm^{-1} and 1259 cm^{-1} for the C=O bond of the carboxyl group and C=O and C–O bonds of the ester group, respectively, but no peaks for the C=O bond of acid chloride (Fig. 2a and S5, ESI†). The result reveals the successful grafting of the chiral D-camphoric acid moiety on TzDa. The modification ratio of D-camphoric acid on TzDA was calculated to be 41% using a toluidine blue O (TBO) dye assay (ESI†).

The powder X-ray diffraction (PXRD) pattern of TzDa prepared *via* the RT approach not only matched well with the simulated PXRD pattern, but also showed all the characteristic peaks of TzDa obtained with the solvothermal approach, indicating the formation of the reported ordered structure of TzDa (Fig. S6, ESI†). All the PXRD peaks of TzDa remained after modification with D-cam-ClO, indicating no change in the crystal structure. The coupling reaction of camphoric acid with its hydroxyl group prevents the formation of intramolecular hydrogen bonds between the hydroxyl groups (Da) on formaldehyde (Tz), which results in a decrease in the crystallinity of the synthesized CTzDa (Fig. 2b and S7, ESI†).

The grafting of D-cam made the zeta potential of COF more negative from −8.2 mV (TzDa) to −47.3 mV (CTaDa) due to the introduction of the hydroxyl group of D-cam (Fig. 2c; Table S1, ESI†). There was no variation in the PXRD patterns and FTIR spectra of CTzDa after immersing in various solvents including tetrahydrofuran (THF), acetonitrile (ACN), dimethyl formamide (DMF), water, 0.1 M HCl and 0.1 M NaOH for 1 day, demonstrating the high chemical stability of CTzDa (Fig. 2d and S8, ESI†). The prepared CTzDa also had high thermal stability up to 200 °C (Fig. S9, ESI†).

The transmission electron microscopy (TEM) images show a layer-like structure for both TzDa and CTzDa and no obvious change in morphology after the grafting of D-camphor acid onto TzDa (Fig. S10, ESI†). The scanning electron microscopy (SEM) images indicate that the surface of CTzDa is rougher than that of TzDa (Fig. S11, ESI†). The Brunauer–Emmett–Teller (BET) surface area and the pore size of TzDa were calculated to be 1380 $m^2 g^{-1}$ and 3.2 nm, respectively, while those of CTzDa decreased to 403 $m^2 g^{-1}$ and 1.8 nm, respectively, due to the introduction of D-camphor acid (Fig. S12 and Table S2, ESI†).

The introduction of a chiral moiety caused various stereoscopic interactions in the COF, which could improve the enantioselective ability of CTzDa. Thus, we employed the synthesized porous material CTzDa for the selective adsorption of chiral AAs (tryptophan (Trp), histidine (His), aspartic acid (Asp) and serine (Ser)). The effect of the concentration of AAs on the adsorption capacity indicated the appropriate concentrations of AAs in adsorption (Fig. S13, ESI†). The effect of pH on the AAs adsorption showed that the adsorption process was favorable near the isoelectric point (Fig. S14, ESI†). In comparison with TzDa, CTzDa exhibited obviously higher enantioselectivity and adsorption capacity to L-AAs than D-AAs (Fig. 3 and S15, ESI†).

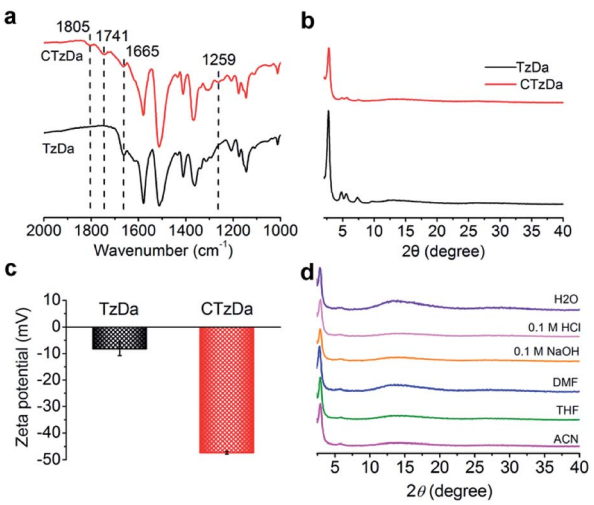

Fig. 2 (a) FTIR spectra of TaDa and CTzDa. (b) PXRD patterns of TaDa and CTzDa. (c) Zeta potential of TzDa and CTzDa. (d) PXRD patterns of CTzDa after immersing in various solvents.

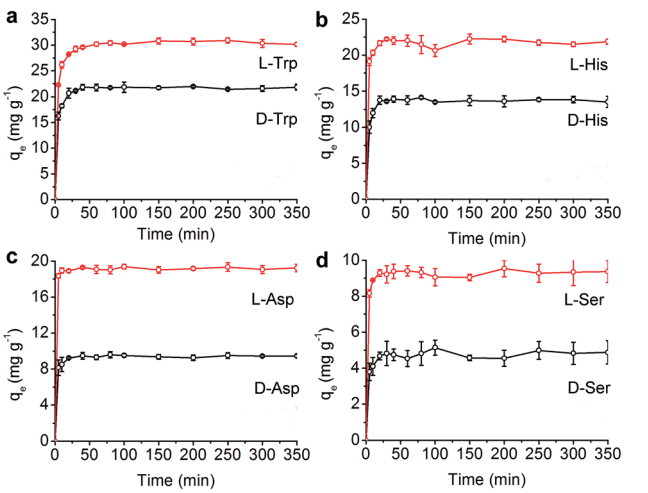

Fig. 3 Time-dependent enantioselective adsorption of AAs on CTzDa at 293 K: (a) D-Trp and L-Trp (50 mg L^{-1}); (b) D-His and L-His (20 mg L^{-1}); (c) D-Asp and L-Asp (red, 20 mg L^{-1}); (d) D-Ser and L-Ser (20 mg L^{-1}).

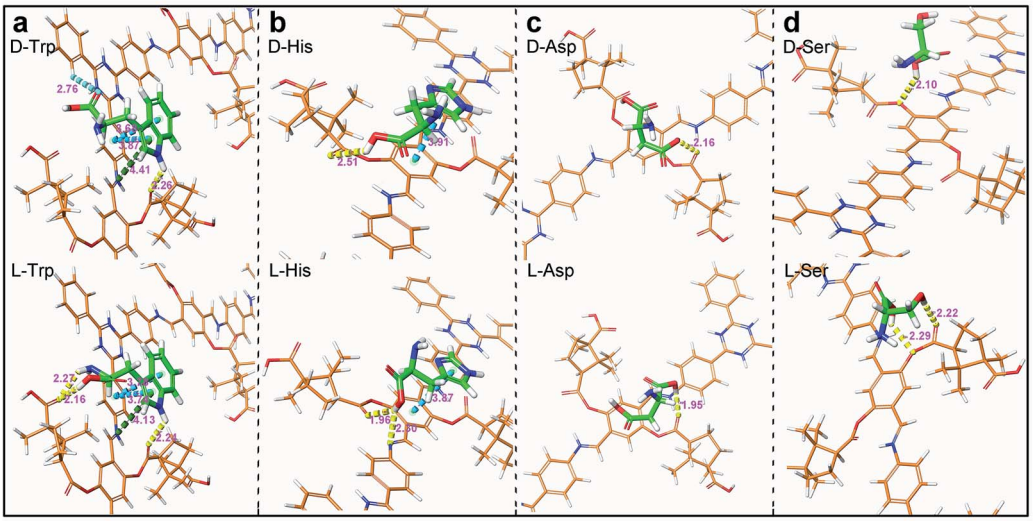

Fig. 4 Molecular docking modes between CTzDa and AAs: (a) Trp; (b) His; (c) Asp; (d) Ser. The receptor COF unit is displayed with thin stick style by marking C in yellow, O in red, N in blue and H in white. The AAs are displayed with thick stick style by marking C in green, O in red, N in blue and H in white. Blue, green and yellow dotted lines represent the π–π interaction, n–π interaction and hydrogen bond between CTzDa and AAs, respectively. Thin figure represents the distance of atoms.

We further investigated the kinetics and adsorption isotherms of AAs on CTzDa. The time-dependent adsorption capacity (q_t) of AAs at three initial concentrations at 293 K showed that the adsorption equilibrium of AAs on CTzDa was achieved within 30 min, indicating the rapid adsorption of AAs on CTzDa (Fig. S16, ESI†). The adsorption followed the pseudo-second-order kinetic model rather than the pseudo-first-order kinetic model (Fig. S17 and S18, ESI†). The larger k_2 values of D-AAs than those of L-AAs indicate different interactions of CTzDa with D-AAs and L-AAs (Table S3, ESI†).[33,34]

The adsorption isotherms were evaluated in an initial concentration range of 10–100 mg L^{-1} at four different temperatures (20–50 °C) (Fig. S19, ESI†). The adsorption isotherms of AAs could be better described by the Langmuir model than the Freundlich model (Table S4, ESI†), indicating monolayer adsorption of AAs on CTzDa. The calculated maximum adsorption capacities (q_m) of L-AAs were higher than those of D-AAs, indicating the selective adsorption of chiral AAs on CTzDa. The adsorption enantioselectivity values of CTzDa were 4.20, 2.59, 2.60 and 1.62 for the enantiomers of Trp, His, Asp and Ser, respectively (Table S5, ESI†). Compared with previous adsorbents, the developed CTzDa exhibited higher enantioselectivity (Table S6, ESI†), showing the great potential of CTzDa as an adsorbent in the enantioselective adsorption of AAs.

Efficient desorption and reusability are essential for adsorbents. Different types of eluents were used for the desorption of AAs from CTzDa at 60 °C under ultrasonication for 5 min (Fig. S20†). The results showed that organic solvents were not favourable for AA desorption. The adsorbed AAs could be well desorbed from CTzDa with water (pH = 4 or 8) (Fig. S20, ESI†) due to the increase in the hydrophilicity of AAs.[35] After five adsorption–desorption cycles, CTzDa exhibited no significant decrease in adsorption capacity, indicating the good reusability of CTzDa for the adsorption of AAs (Fig. S21, ESI†). There was no obvious change in the PXRD pattern and FTIR spectra after five adsorption–desorption cycles, suggesting that CTzDa was stable during adsorption and desorption (Fig. S22, ESI†).

The adsorption thermodynamics was assessed by the change in Gibbs free energy (ΔG), enthalpy (ΔH) and entropy (ΔS) (Fig. S23, S24 and Table S7, ESI†). The negative ΔG value indicated that the adsorption of AAs on CTzDa was thermodynamically spontaneous. The negative ΔH value suggested the presence of an exothermic process, which was related to the decrease in adsorption capacity at high temperatures. The negative ΔS value demonstrated the AAs lost freedom during the adsorption process.

AutoDock Vina (ADVina) was used to perform docking calculations.[36,37] The calculated binding energy (BE, kcal mol^{-1}) represents the generated energy in adsorption (Table S8, ESI†). The existing interaction modes between CTzDa and AAs are shown in Fig. 4. The binding interactions between AAs and the building unit mainly included π–π interactions, C–H···π interactions and H-bonds, but the strengths related to the stereoscopic interactions were different, which originally resulted in distinct adsorptions. For Trp, the carboxyl and amino groups of L-Trp could both form hydrogen bonds with CTzDa, while the different stereoscopic positions of D-Trp led to only carboxyl group forming aromatic H-bonds with CTzDa (Fig. 4a). The carboxyl group of L-His or L-Ser formed hydrogen bonds with CTzDa. On the contrary, the corresponding hydrogen bond of D-His or D-Ser between the carboxyl group and CTzDa was absent due to the large distance (Fig. 4b and d). The hydrogen bond length between L-Asp and CTzDa (1.95 Å) was shorter than that between D-Asp and CTzDa (2.61 Å) (Fig. 4c). The above-mentioned different stereoscopic interactions made the BE between the main framework and racemic AAs follow the order L-AAs > D-AAs, indicating the stronger adsorption of L-AAs than that of D-AAs on CTzDa (Table S8†). The K_L/K_D ratios were 1.97, 1.66, 1.18 and 1.40 for Trp, His, Aps and

Ser, respectively. $K_L/K_D > 1$ also indicated that CTzDa exhibited stronger adsorption of L-AAs than that of D-AAs.

In summary, we have designed and synthesised the chiral COF CTzDa through introducing a chiral selector (D-cam) in the COF TzDa at room temperature in a facile manner. The prepared CTzDa showed good stability in various solvents, which was favourable for adsorption. CTzDa also exhibited rapid kinetics and high selectivity for the adsorption separation of the enantiomers of amino acids. Docking calculations showed that the difference in the stereoscopic hydrogen bonds between L-AAs and D-AAs is the key interaction for the enantioselective adsorption of AAs on CTzDa. This work provides a facile strategy for highly selective adsorption of AA enantiomers. Further research will focus on the potential of CTzDa in the chiral chromatographic separation of AAs.

Conflicts of interest

There are no conflicts to declare.

Acknowledgements

This work was supported by the National Natural Science Foundation of China (No. 21775056 and 21804055), the Natural Science Foundation of Jiangsu Province (No. BK20180585), the National First-class Discipline Program of Food Science and Technology (No. JUFSTR20180301), the Fundamental Research Funds for the Central Universities (JUSRP51714B), the Program of "Collaborative Innovation Center of Food Safety and Quality Control in Jiangsu Province".

Notes and references

1 A. Higuchi, M. Tamai, Y.-A. Ko, Y.-I. Tagawa, Y.-H. Wu, B. D. Freeman, J.-T. Bing, Y. Chang and Q.-D. Ling, *Polym. Rev.*, 2010, **50**, 113–143.
2 X. Li, C. Meng, Y. Meng, L. Gu, Q. Chen and H. Liu, *Colloids Surf., A*, 2019, **581**, 123789.
3 V. Sojo, *Origins Life Evol. Biospheres*, 2015, **45**, 219–224.
4 G. D. Tarigh and F. Shemirani, *Talanta*, 2015, **144**, 899–907.
5 X. Han, J. Huang, C. Yuan, Y. Liu and Y. Cui, *J. Am. Chem. Soc.*, 2018, **140**, 892–895.
6 W.-T. Kou, C.-X. Yang and X.-P. Yan, *J. Mater. Chem. A*, 2018, **6**, 17861–17866.
7 B. Chen, J. Deng and W. Yang, *Adv. Funct. Mater.*, 2011, **21**, 2345–2350.
8 I. Weissbuch and M. Lahav, *Chem. Rev.*, 2011, **111**, 3236–3267.
9 A. Holbach, S. Soboll, B. Schuur and N. Kockmann, *Ind. Eng. Chem. Res.*, 2015, **54**, 8266–8276.
10 Y. Ohishi, M. Murase, H. Abe and M. Inouye, *Org. Lett.*, 2019, **21**, 6202–6207.
11 X. Wang, X. Wang, M. Wang, D. Zhang, Q. Yang, T. Liu, R. Lei, S. Zhu, Y. Zhao and C. Chen, *Small*, 2018, **14**, e1703982.
12 X. Hou, T. Xu, Y. Wang, S. Liu, R. Chu, J. Zhang and B. Liu, *ACS Appl. Mater. Interfaces*, 2018, **10**, 26365–26371.
13 Y. Z. H. Lu, H. C. Zhang, J. Y. Chan, R. W. Ou, H. J. Zhu, M. Forsyth, E. M. Marijanovic, C. M. Doherty, P. J. Marriott, M. M. B. Holl and H. T. Wang, *Angew. Chem., Int. Ed.*, 2019, **58**, 16928–16935.
14 L. Chen, P. S. Reiss, S. Y. Chong, D. Holden, K. E. Jelfs, T. Hasell, M. A. Little, A. Kewley, M. E. Briggs, A. Stephenson, K. M. Thomas, J. A. Armstrong, J. Bell, J. Busto, R. Noel, J. Liu, D. M. Strachan, P. K. Thallapally and A. I. Cooper, *Nat. Mater.*, 2014, **13**, 954–960.
15 E. Faggi, C. Vicent, S. V. Luis and I. Alfonso, *Org. Biomol. Chem.*, 2015, **13**, 11721–11731.
16 J. Janczak, D. Prochowicz, J. Lewinski, D. Fairen-Jimenez, T. Bereta and J. Lisowski, *Chem.–Eur. J.*, 2016, **22**, 598–609.
17 S. A. Boer, K. F. White, B. Slater, A. J. Emerson, G. P. Knowles, W. A. Donald, A. W. Thornton, B. P. Ladewig, T. D. M. Bell, M. R. Hill, A. L. Chaffee, B. F. Abrahams and D. R. Turner, *Chem.–Eur. J.*, 2019, **25**, 8489–8493.
18 T. Chen, H. Tan, Q. Chen, L. Gu, Z. Wei and H. Liu, *ACS Appl. Mater. Interfaces*, 2019, **11**, 48402–48411.
19 K. Zhang, S. L. Cai, Y. L. Yan, Z. H. He, H. M. Lin, X. L. Huang, S. R. Zheng, J. Fan and W. G. Zhang, *J. Chromatogr. A*, 2017, **1519**, 100–109.
20 H. L. Qian, C. X. Yang, W. L. Wang, C. Yang and X. P. Yan, *J. Chromatogr. A*, 2018, **1542**, 1–18.
21 S. N. Zhang, Y. L. Zheng, H. D. An, B. Aguila, C. X. Yang, Y. Y. Dong, W. Xie, P. Cheng, Z. J. Zhang, Y. Chen and S. Q. Ma, *Angew. Chem., Int. Ed.*, 2018, **57**, 16754–16759.
22 X. L. Huang, H. H. Lan, Y. L. Yan, G. Chen, Z. H. He, K. Zhang, S. L. Cai, S. R. Zhen, J. Fan and W. G. Zhang, *Sep. Sci. plus*, 2019, **2**, 120–128.
23 J. Zhang, X. Han, X. Wu, Y. Liu and Y. Cui, *J. Am. Chem. Soc.*, 2017, **139**, 8277–8285.
24 L. Zhu and Y. B. Zhang, *Molecules*, 2017, **22**, 1149.
25 M. Li, Z. Cui, S. Pang, L. Meng, D. Ma, Y. Li, Z. Shi and S. Feng, *J. Mater. Chem. C*, 2019, **7**, 11919–11925.
26 J. Wang and B. Yan, *Anal. Chem.*, 2019, **91**, 13183–13190.
27 L. Chen, K. Furukawa, J. Gao, A. Nagai, T. Nakamura, Y. Dong and D. Jiang, *J. Am. Chem. Soc.*, 2014, **136**, 9806–9809.
28 X. Chen, M. Addicoat, E. Jin, L. Zhai, H. Xu, N. Huang, Z. Guo, L. Liu, S. Irle and D. Jiang, *J. Am. Chem. Soc.*, 2015, **137**, 3241–3247.
29 Z. L. Li, H. Li, X. Y. Guan, J. J. Tang, Y. R. Yusran, Z. Li, M. Xue, Q. R. Fang, Y. S. Yan, V. Valtchev and S. L. Qiu, *J. Am. Chem. Soc.*, 2017, **139**, 17771–17774.
30 H. W. Fan, J. H. Gu, H. Meng, A. Knebel and J. Caro, *Angew. Chem., Int. Ed.*, 2018, **57**, 4083–4087.
31 H. L. Qian, C. X. Yang and X. P. Yan, *Nat. Commun.*, 2016, **7**, 12104.
32 H. L. Qian, C. Dai, C. X. Yang and X. P. Yan, *ACS Appl. Mater. Interfaces*, 2017, **9**, 24999–25005.
33 B. Pan, P. Huang, M. Wu, Z. Y. Wang, P. Wang, X. C. Jiao and B. S. Xing, *Bioresour. Technol.*, 2012, **103**, 367–373.
34 J. H. Franke and D. S. Kosov, *J. Chem. Phys.*, 2015, **142**, 7.
35 S. D. Black and D. R. Mould, *Anal. Biochem.*, 1991, **193**, 72–82.
36 E. Zor, M. Esad Saglam, S. Alpaydin and H. Bingol, *Anal. Methods*, 2014, **6**, 6522–6530.
37 E. Zor, H. Bingol, A. Ramanaviciene, A. Ramanavicius and M. Ersoz, *Analyst*, 2015, **140**, 313–321.

